Simulation of the tropical intraseasonal oscillation with a coupled ocean-atmosphere general circulation model

Silvio Gualdi

INGV, Bologna, Italy

Abstract

In this study we report the simulation of the intraseasonal oscillation of the tropical atmosphere, also known as Madden-Julian Oscillation (MJO), in a coupled general circulation model (CGCM). Over the Indian Ocean and Indonesian archipelago, the model produces an eastward propagating disturbance, which is in good agreement with many aspects of the observed oscillation. During its propagation, the simulated MJO seems to reproduce the basic air-sea interaction mechanisms which characterize the observed disturbance. Low-level moisture convergence mechanism for eastward propagation seems to be active across the Indian Ocean-Indonesian region. The simulated MJO, on the other hand, exhibits substantial problems in propagating across the western Pacific. Unlike the observations, the model does not exhibits a coherent propagation of convective anomalies over the warm pool, while it tends to produce a standing oscillation of convection near the date-line. These weaknesses in the model MJO appear to be linked to systematic error of the mean state, consistent with other model results (Innes and Slingo 2003).

1. Introduction

Recent observational studies (e.g., Lau and Sui 1997, Woolnough et al. 2000, Sperber 2003) show that air-sea interactions might play an important role in the development and in the maintenance of the tropical intraseasonal oscillation (Madden and Julian 1994, for a general review). These observational evidences and the difficulties faced by purely atmospheric models (Slingo et al. 1996, Sperber et al. 1997) have led to the suggestion that the oscillation may be regarded as a coupled ocean-atmosphere mode, where the MJO convective systems interact with the sea-surface temperature (SST) and surface fluxes, producing changes in the local distribution of the surface fields. These changes, in turn, favor the eastward propagation of the convective disturbances (Sperber et al. 1997, Flatau et al. 1997, Waliser 1999, Woolnough et al. 2000).

Additionally, recent model studies indicate that the simulation of the MJO with coupled atmosphere-ocean models exhibits improvements compared to the oscillation produced with the atmosphere-only models (Gualdi et al. 1999, Waliser et al. 1999, Innes and Slingo 2003).

Although during the last few years a variety of fully-coupled ocean-atmosphere model (CGCMs) have been developed, the documentation of the capability of the CGCMs to simulate the tropical intraseasonal variability is still rather poor. The first aim of this work is to investigate and to assess the skill of a CGCM to reproduce the MJO.

2. Model and methodology

The model used in this study is a coupled ocean-atmosphere model, known as SINTEX (Gualdi et al. 2003, Guilyardi et al. 2003), where atmosphere and ocean exchange fluxes without any correction. The atmospheric component is formed by the ECHAM-4 model (Roeckner et al. 1996) at horizontal resolution triangular 106 (T106), with 19 vertical levels. When forced with observed SST, ECHAM-4 appears to reproduce a MJO-like variability (Gualdi and Navarra 1998). The ocean component is formed by the OPA-8.1 model (Madec et al. 1998), OPA is used with a zonal resolution of 2° and a meridional resolution that decreases from about 0.5°. at the equator to about 2° at the northern and southern boundaries. The coupling

interface is OASIS 2.4 (Valke et al. 2000). In this study, we present results obtained from a 100-year year coupled integration. As validation data, we use the NCEP/NCAR reanalysis (Kalnay et al. 1996) and AVHRR OLR (Liebmann and Smith 1996) for the period 1979-2002.

A 20-100 day band-pass filter has been applied to all the data in order to highlight the intraseasonal time scales. The MJO signal has been identified by means of an Empirical Orthogonal Function (EOF) analysis applied to the 20-100 band-pass filtered OLR anomalies over the region 45°E-120°W, 20°S-20°N, for the period November-March. The EOF Principal Components (PCs) have been used to define an index of the oscillation, which, in turn, has been used to construct composite patters of various fields. In order to select eastward propagating convective events associated with the MJO activity, we used the selection criteria defined and discussed in Woolnough et al. (2000) and Innes and Slingo (2003).

3. Results

The simulated mean SST are shown in Fig.1, left panel. When compared with the observations (right panel), the simulated SST climatology exhibits a cold bias in the Tropics and in the Mid-latitudes. However, in the up-welling regions off the American coast, the Gulf of Guinea and in the eastern part of the equatorial cold tongue, the model is too warm. The equatorial cold tongue penetrates too far into the west Pacific and the SST patterns are too much symmetrical around the equator, especially south of the equator, eastward of the date line, the SSTs are too much zonally oriented. There is a tendency to simulate a double ITCZ, as shown by the simulated mean precipitation (not shown), with an excess of convective activity over the subtropical eastern Pacific.

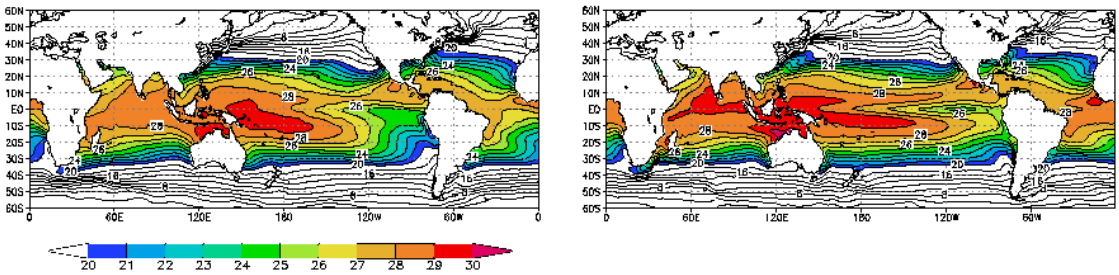

Figure 1 Mean November-March Sea-Surface Temperature (SST) as obtained from the observations (HadISST, left panel) and from the model (right panel). Contour interval is 1°C.

The observed near-surface mean wind (Figure 2, left panel) is predominantly easterly over most of the tropical belt. However, the near-equatorial Indian Ocean and West Pacific are characterized by a broad region of westerlies. The model (Figure 2, right panel) reproduces the basic features of the observations, but with the notable difference of the western Pacific. In this region, in contrast with the observations, the model mean state is characterized by surface easterlies. This model shortcoming might be important for the eastward propagation of the intraseasonal convection, as suggested by Innes and Slingo (2003).

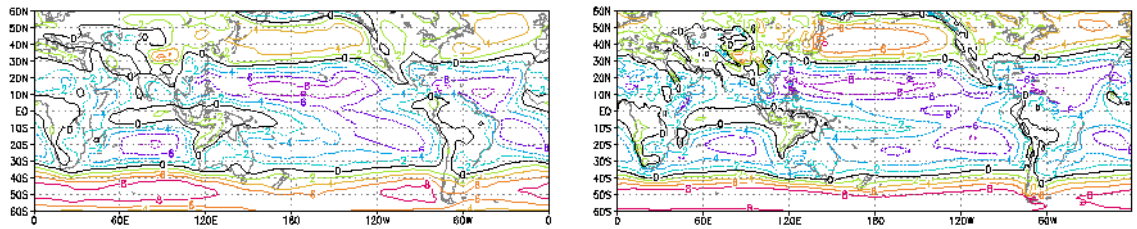

Figure 2 Mean November-March near-surface (1000hPa) zonal wind as obtained from the NCEP/NCAR reanalysis (left panel) and from the model (right panel). Contour interval is 2 m/s.

The EOF analysis applied to the band-pass filtered time series of simulated OLR anomaly has identified two dominant modes of variability which explain about 50% of the total intraseasonal variance over the Indian Ocean and Indonesian region (Figure 3). The dominant EOF patterns appear to be shifted of about 90°, and when combined with the respective PCs (not shown) they describe an eastward propagating convective disturbance. The maximum correlation between PC1 and PC2 is obtained for a lag of 9 days, indicating that the convective disturbance develops over the Indian Ocean and then propagate eastward to the western Pacific in about 36 days.

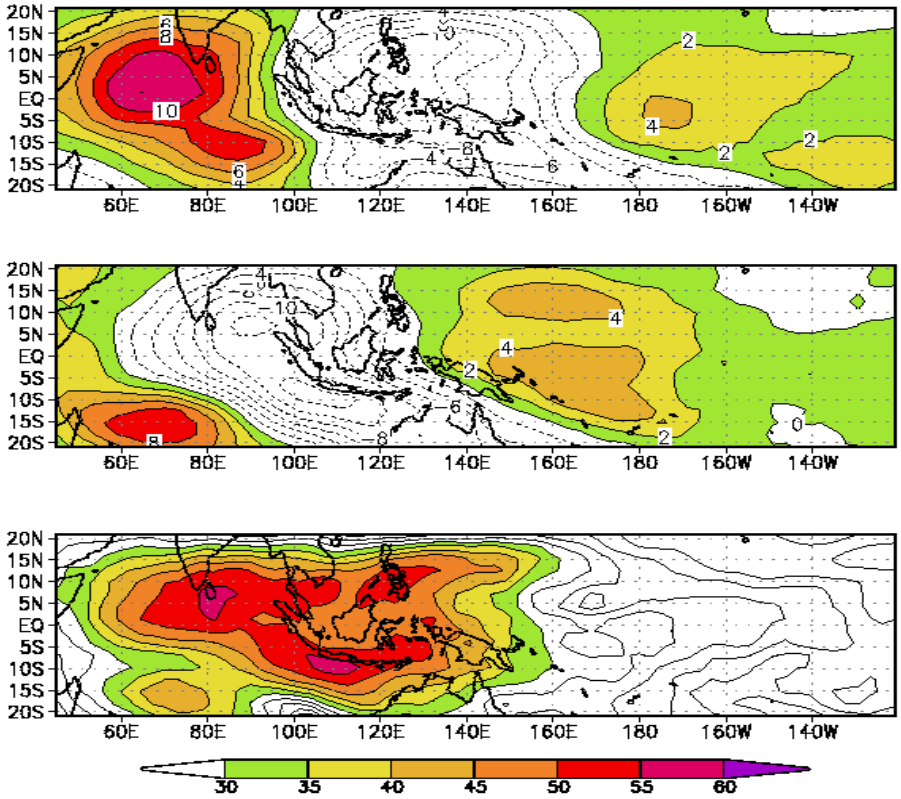

Figure 3 EOF patterns of the simulated intraseasonal (20-100-day band-pass filtered) OLR anomaly. Upper panel: first mode (EOF1); middle panel: second mode (EOF2); lower panel percentage of the intraseasonal variance explained by EOF1 and EOF2.

Figure 4 shows the composite patterns of equatorial (10°S-10°N) OLR anomalies associated with the MJO cycle as detected by the index based on PC1. The composites are shown in form of longitude-time diagrams. The model (right panel) represents reasonably well the eastward propagation of the convective anomaly, associated with the MJO, from the central-western equatorial Indian Ocean to the Maritime continent. In the observations (Figure 4, left panel), the convective anomaly propagates across the western Pacific reaching the date line. In the model, the propagation over the West Pacific is less coherent, and the signal found over the date line appears more as a standing oscillation.

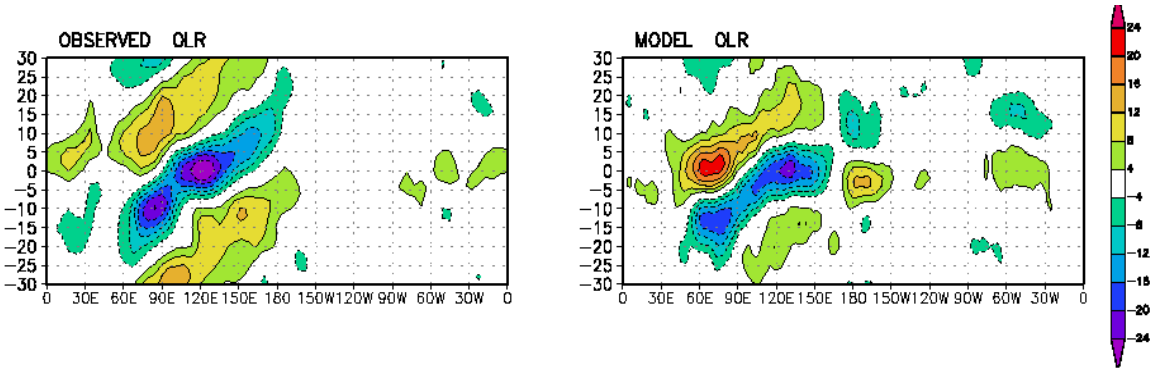

Figure 4 Time-longitude diagram of the composite patters of the observed (left panel) and simulated (right panel) OLR anomaly. The composites have been computed using a MJO index based on the EOF PC1, as described in the text. The anomalies have been averaged between 10°S and 10°N. The time lag (y-axis) is in days. Lag 0 corresponds to the maximum of MJO convection anomaly over the Maritime Continent (about 120°E). Contour interval is 4 W/m^2.

In Figure 5 the composite of the OLR anomaly (contour pattern) is shown together with the composites obtained for precipitation, SST, surface solar radiation (SSR) and near-surface zonal wind anomalies (shaded patters). Both the anomalies of precipitation and SSR are coherently related with the OLR anomaly. These fields propagate in phase across the Indian ocean, indicating that the convective signal is associated with a substantial perturbation of both rainfall and SSR.

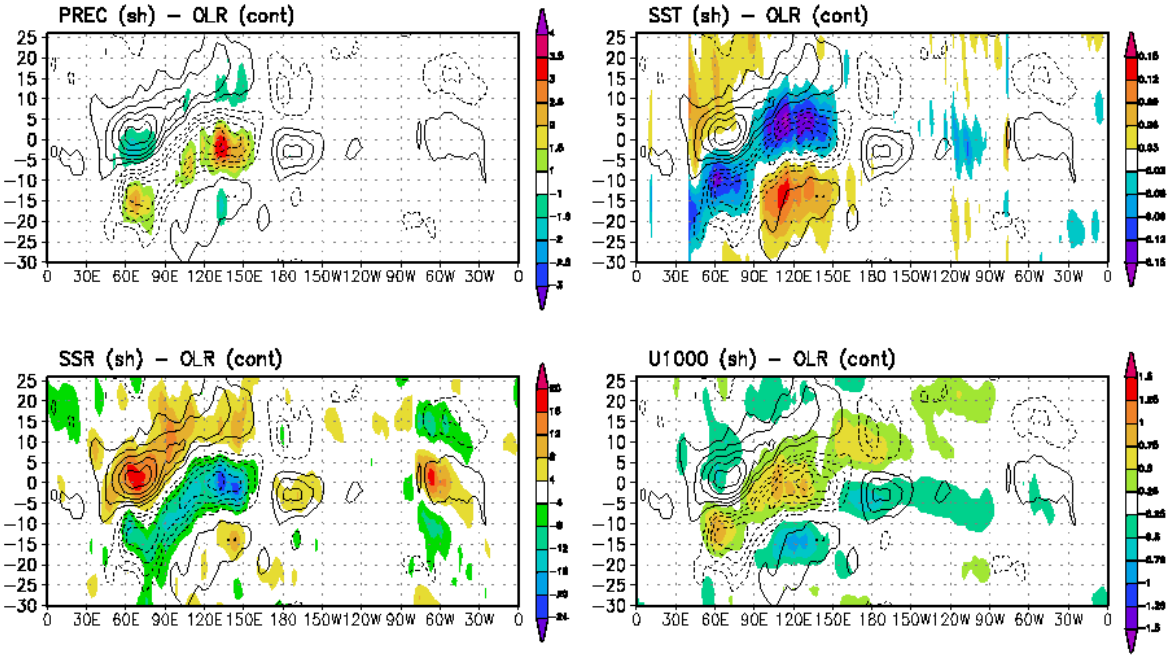

Figure 5 Time-longitude diagram of the composite patters of the simulated OLR (contour, all panels), precipitation (shaded, upper-left panel), surface solar radiation flux (SSR, shaded, lower-left panel), sea-surface temperature (SST, shaded, upper-right) and near-surface zonal wind (u1000, shaded, lower-right panel) anomalies. Contour intervals are: OLR, 4 W/m^2; precipitation, 0.5 mm/day; SST, 0.03 °C; SSR, 4 W/m^2; u1000, 0.25 m/s.

The intraseasonal SST anomalies (Figure 5, upper-right panel) are small, but their magnitude is comparable to the results found in similar studies (e.g., Waliser et al. 1999, Innes and Slingo 2003) . Over the Indian Ocean and the warm pool, the SST anomalies show a clear tendency to propagate eastward and their modulation appears to be coherently related with precipitation and surface short-wave flux anomalies. The SSR anomalies generally lead the SST anomalies, which, in turn, tend to lead the OLR and precipitation

anomalies. In agreement with the observations (Woolnough et al. 2000), warm (cold) SST anomalies are found to the east (west) of the convection. The near-surface zonal wind composite (Figure 5, lower-right panel) indicates that the warm SST develops in correspondence of surface easterly anomalies, whereas the cold SST anomaly occurs during surface westerly anomalies. Also in agreement with the observational results, the highest magnitude of wind anomalies are generally found slightly west of the OLR anomalies; whereas east of the convective anomalies the wind anomalies tend to have smaller magnitude.

The strength and the structure of the wind anomalies at the top of the troposphere (not shown) and near the surface (Figure 5, lower-right panel) are similar to the results found from analyses (Gualdi et al. 1997), even though the simulated anomalies over the Indian Ocean appear to be slightly underestimated.

The near-surface moisture divergence (QDIV) anomaly (Figure 6, left panel observations; right panel model) appears to lead the OLR anomaly. In the equatorial Indian Ocean, the convective disturbance starts to develop in correspondence of near-surface moisture convergence, between time-lag -25 and -20 days. After a few days, moisture convergence anomalies start to develop at about 40°-60° to the east of convection. The phase relationship between OLR and QDIV suggests that, both in the model and in the observations, the eastward propagation of convection is favored by near-surface convergence of moist flow.

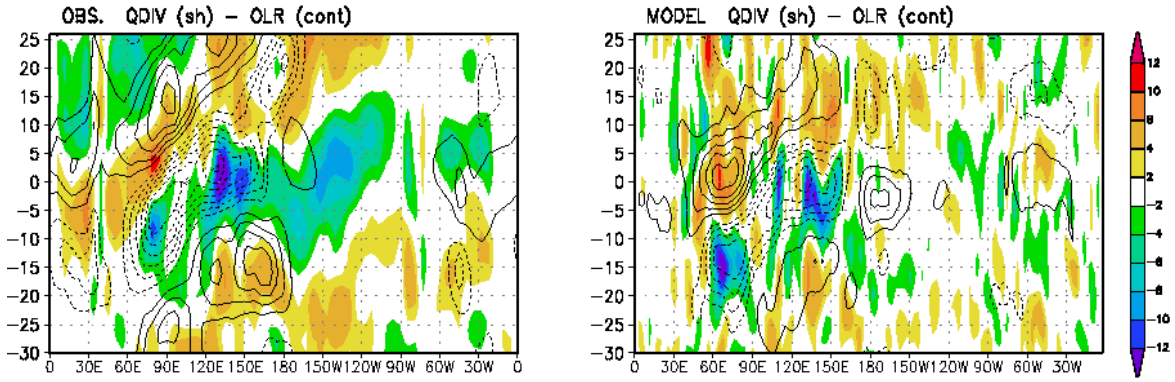

*Figure 6 As Figure 5 but for OLR (contour) and near-surface (1000 hPa) moisture divergence (QDIV, shaded patterns). Left panel, observations and re-analysis; right panel model results. Contour interval: OLR (contour): 4 W/m^2; QDIV (shaded): 1.e+6 g/(Kg*s).*

In order to assess a possible impact of the atmospheric model resolution onto the simulated MJO, a similar analysis has been computed for a coupled run carried out with a lower resolution of the atmospheric component. The only difference between the high-resolution (T106) and the low-resolution (T30) run is the triangular truncation of the atmospheric model, which occurs at wave-number 106 and wave-number 30 respectively. In the two cases, the ocean component is exactly the same.

The basic features of the MJO simulated with the low-resolution model (not shown) are very similar to the high resolution case. This result, consistent with Gualdi et al. (1997), suggests that the increase of the atmospheric horizontal resolution does not lead to substantial improvements of the simulated MJO.

4. Summary

Over the Indian Ocean and Indonesian region, the coupled model SINTEX produces an eastward propagating disturbance with characteristics similar to the observed MJO. In this region, the simulated oscillation appears as a propagating convection anomaly associated with anomalies of precipitation, SST, surface wind. The phase relationship between these fields indicate that the model reproduces the basic air-sea interaction mechanisms found in the observations. Low-level moisture convergence anomalies develop in correspondence and to the east of the convection centre. The phase relationship between moisture divergence

and convective anomalies obtained from the model is consistent with the observational results, and suggests that the eastward propagation of convection is favored by near-surface convergence of moist flow.

In contrast with the observations, the simulated MJO exhibits difficulties in propagating across the western Pacific. The model deficiency to simulate a coherent propagation of convection over the warm pool is consistent with the results obtained with other coupled models, and might be related with the systematic error of the mean state, as discussed in Innes and Slingo (2003).

The impact of the atmospheric horizontal resolution onto the simulation of the MJO has been assessed analyzing the results obtained from two coupled experiments performed with different resolution of the atmospheric component. The characteristics of the MJO simulated with the two versions of the model are very similar. In particular, the lack of propagation of the convective signal over the western Pacific is evident both at low and high resolution, indicating that some of the physical processes responsible for the MJO are still elusive in this formulation of the model.

References

Flatau, M., P. J. Flatau, P. Phoebus, and P.P. Niiler, 1997: The feedback between equatorial convection and local radiative and evaporative processes: the implications for intraseasonal oscillations, *J. Atmos. Sci*., **54**, 2373-2386.

Gualdi, S., A. Navarra and H. von Storch, 1997: Tropical intraseasonal oscillation appearing in operational analyses and in a family of general circulation models, *J. Atmos. Sci*., **54**, 1185-1202.

Gualdi, S., A. Navarra, and M. Fischer, 1999: The tropical intraseasonal oscillation in a coupled GCM. *Geophys. Res. Lett.*, **26**, 2973-2976.

Gualdi, S., and A. Navarra, 1998: A study of the seasonal variability of the tropical intraseasonal oscillation. *The Global Atmos. and Ocean System*, **6**, 337-372.

Gualdi, S., E. Guilyardi, A. Navarra, and P. Delecluse, 2003: Assessment of the Tropical Indo-Pacific climate in the SINTEX CGCM. *Ann. Geophys*., **46**, 1-26.

Guilyardi, E., P. Delecluse, S. Gualdi, and A. Navarra, 2003: Mechanisms for ENSO phase change in a coupled GCM. *J. Climate*, **16**, 1141-1158.

Innes, P. M. and J. M. Slingo, 2003: Simulation of the Madden-Julian Oscillation in a coupled general circulation model. Part I: comparison with observations and an atmosphere-only GCM. *J. Climate* **16**, 365-382

Kalnay, E. M., and Co-authors, 1996: The NCEP/NCAR 40-year re-analysis project. *Bull. Amer. Met. Soc*., **77**, 437-471.

Lau, K. M., and C. H. Sui, 1997: Mechanisms of short-term seas surface temperature regulation: observations during TOGA-COARE. *J. Climate*, **9**, 465-472.

Liebmann, B. and C. A. Smith, 1996: Description of a complete (interpolated) OLR dataset. *Bull. Amer. Met. Soc.*, **77**, 1275-1277.

Madden, R. A., and P. R. Julian, 1994: Observations of the 40-50 day tropical oscillation- A review, *Mon. Wea.Rev*., **122**, 814-837.

Madec, G., P. Delecluse, M. Imbard, and C. Levy, 1998: OPA version 8.1, ocean general circulation model reference manual. *Technical Report, LODYC/IPSL*, Note 11, Paris, France, pp. 91.

Roeckner, E., and Co-authors, 1996: The atmospheric general circulation model Echam-4: model description and simulation of present-day climate. *Max Planck-Institut fuer Meteorologie Report* No 218, 90 pp., Hamburg, Germany.

Sperber, K. R., J. M. Slingo, P. M. Innes, and, W. K-M. Lau, 1997: On the maintenance and initiation of the intraseasonal oscillation in the NCEP/NCAR reanalysis and in the GLA and UKMO AMIP simulations, *Clim Dyn.,* **13**, 769-795.

Sperber, K. R., 2003: Propagation and the vertical structure of the Madden-Julian Oscillation. *Mon. Wea. Rev*., in press.

Valcke, S., L. Terray, and A. Piacentini, 2000: The OASIS coupler user guide version 2.4. *Technical Report, TR/CMGC/00-10, CERFACS*, Toulouse, France, 85 pp.

Waliser E. D., K. M. Lau and J.-H. Kim, 1999: The influence of coupled Sea Surface Temperatures on the Madden--Julian oscillation: a model perturbation experiment, *J. Atmos. Sci*., **56**, 333-358.

Woolnough, S. J., J.M. Slingo, and B. J. Hoskins, 2000: The relationship between convection and sea-surface temperature on intraseasonal time scales. *J. Climate*, **13**, 2086-2104.